

Cambridge, Mass.
May 20, 1947

Professor G. W. Swett
Secretary of the Faculty
Massachusetts Institute of Technology
Cambridge, Massachusetts

Dear Sir:

In accordance with the requirements for the degree of Master of Science in Mechanical Engineering, I submit herewith a thesis entitled "Friction Factors for Turbulent Flow in the Transition Region for Straight Tubes".

Respectfully,

Robert Douglas Smith

FRICION FACTORS FOR TURBULENT FLOW IN TRANSITION
REGION FOR STRAIGHT TUBES

by

Robert Douglas Smith
B.S. in M.E., Tufts College, 1945

SUBMITTED IN PARTIAL FULFILLMENT OF REQUIREMENTS FOR
THE DEGREE OF MASTER OF SCIENCE IN MECHANICAL ENGINEERING

at the

Massachusetts Institute of Technology
1947

Signature of Author

Department of Mechanical Engineering
May 20, 1947

Signature of Instructor in charge of research

Signature of Chairman of Department
Committee on Graduate Students

ACKNOWLEDGEMENTS

The author wishes to thank Professor Ascher H. Shapiro of the Department of Mechanical Engineering, Massachusetts Institute of Technology, for suggesting the problem undertaken as a thesis subject, and for his suggestions as to the method of attack. Mr. Dumont Rush of the D.I.C. Staff of the Institute was of invaluable assistance, yielding the benefit of considerable research experience as well as material aid.

Professor Shapiro made available data taken by himself on this same project, and full benefit of his experience in obtaining this data resulted in numerous improvements on the method of attack.

To Professor Shapiro sincere appreciation is extended for his review and criticism of this thesis prior to its final submission.

TABLE OF CONTENTS

PAGE

I.	ABSTRACT	1
II.	PURPOSE	3
III.	STATUS OF THE PROBLEM	4
IV.	CHOICE AND DESCRIPTION OF METHODS	7
V.	DESCRIPTION OF APPARATUS	10
VI.	THEORY OF REFLECTION FACTOR CALCULATIONS	14
VII.	CALCULATIONS	17
VIII.	DISCUSSION AND CONCLUSIONS	17
LX	DATA	25
X.	BIBLIOGRAPHY	62
	APPENDIX I	66
	APPENDIX II	68

TABLE OF PHOTOGRAPHS AND DIAGRAMS

Following
Page No.

Page

View 1-	General Front View of Water Flow Apparatus-----	66
View 2-	General End View of Water Flow Apparatus-	67
Figure 1-	Schematic View Original Water Flow Test Apparatus-----	5
Figure 2-	Schematic Diagram of Water Manometer Panel-	12
Figure 3-	Schematic Diagram of Mercury Manometer Panel-----	12
Figure 4-	Calming Chamber Assembly-----	
Figure 5-	Distributor Baffle for Calming Chamber-----	
Figure 6-	Distributor Baffle for Calming Chamber ----	9
Figure 7-	Honeycomb for Calming Chamber -----	9
Figure 8-	Flange of Calming Chamber -----	9
Figure 9-	Details .755 inch tube -----	12
Figure 10-	Entrance Nozzle .755 inch tube -----	12
Figure 11-	Exit Nozzle .735 inch tube -----	6
Figure 12-	Entrance Nozzle .573 inch tube -----	6
Figure 13-	Exit Nozzle .373 inch tube -----	6
Figure 14-	Schematic View Air Flow Apparatus -----	10
Figure 15-	Entrance Flange .373 inch tube -----	10
Figure 16-	Flow of Water in Smooth Tubes no initial turbulence low Reynolds Number friction factor versus X/D -----	18
Figure 17-	Flow of Water in Smooth Tubes no initial turbulence low Reynolds number - log f versus log Reynolds \times -----	18

- Figure 18 - Flow of Water in Smooth Tubes no initial turbulence high Reynolds Number ratio of friction factors versus X/D . ----- 18
- Figure 19 - Flow of Water in Smooth Tubes no initial turbulence high Reynolds Number \log Reynolds $_x$ - 18
- Figure 20 - Flow of Water in Smooth Tubes (screen at inlet), low Reynolds Number - ratio of friction factors versus X/D . ----- 18
- Figure 21 - Flow of Water in Smooth Tubes (screen at inlet, low Reynolds Number) - $\log f$ versus \log Reynolds $_x$ ----- 18
- Figure 22 - Flow of Water in Smooth Tubes (screen at inlet, high Reynolds Number) - ratio of friction factors versus X/D ----- 18
- Figure 23 - Flow of Water in Smooth Tubes (screen at inlet, high Reynolds Number) - $\log f$ versus \log Reynolds $_x$ ----- 18
- Figure 24 - Flow of air in Smooth Tubes (no initial Turbulence, low Reynolds Number) - ratio of friction factors versus X/D ----- 18
- Figure 25 - Flow of Air in Smooth Tubes (no initial turbulence, low Reynolds Number) - $\log f$ versus \log Reynolds $_x$ ----- 8
- Figure 26 - Flow of Air in Smooth Tubes (no initial turbulence, high Reynolds Number) - ratio of friction factors versus X/D ----- 18
- Figure 27 - Flow of Air in Smooth Tubes (no initial turbulence, high Reynolds Number) - $\log f$ versus \log Reynolds $_x$ ----- 18
- Figure 28 - Flow of air in Smooth Tubes (screen at inlet, low Reynolds Number) - ratio of friction factors versus X/D ----- 18
- Figure 29 - Flow of air in Smooth Tubes (screen at inlet. low Reynolds Number) - $\log f$ versus \log Reynolds $_x$ ----- 18
- Figure 30 - Flow of Air in Smooth Tubes (screen at inlet, high Reynolds Number) - ratio of friction factors versus X/D ----- 18

- Figure 31 - Flow of Air in Smooth Tubes (screen at inlet, high Reynolds Number) - log f versus log Reynolds_x ----- 18
- Figure 32 - Flow of Air in Smooth Tubes - (snowing range of values, no initial turbulence) - log f versus log Reynolds_x ----- 19
- Figure 33 - Flow of Air in Smooth Tubes - (snowing idealized curve) - log f versus log Reynolds_x ----- 19
- Figure 34 - Flow of Water in Smooth Tubes - (effect of Reynolds_D, no initial turbulence) - ratio of friction factors versus X/D ----- 19
- Figure 35 - Flow of Water in Smooth Tubes (effect of Reynolds_D, no initial turbulence) - log f versus log Reynolds_x ----- 19
- Figure 36 - Flow of Air in Smooth Tubes (effect of Reynolds_D, no initial turbulence) - ratio of friction factors versus X/D ----- 19
- Figure 37 - Flow of Air in Smooth Tubes (effect of Reynolds_D, no initial turbulence) - log f versus log Reynolds_x ----- 19
- Figure 38 - Flow of Air in Smooth Tubes (effect of Reynolds_D, no initial turbulence) - ratio of friction factors versus X/D ----- 19
- Figure 39 - Flow of Air in Smooth Tubes (effect of Reynolds_D, no induced turbulence) - log f versus log Reynolds_x ----- 19
- Figure 40 - Flow of Water in Smooth Tubes (effect of Reynolds_D, no induced turbulence) - ratio of friction factors versus X/D ----- 19
- Figure 41 - Flow of Water in Smooth Tubes (effect of Reynolds_D, no induced turbulence) - log f versus log Reynolds_x ----- 19
- Figure 42 - Flow of Air in Smooth Tubes (effect of Reynolds_D, screen at inlet) - ratio of friction factors versus X/D ----- 19
- Figure 43 - Flow of Air in Smooth Tubes (effect of Reynolds_D, screen at inlet - log f versus log Reynolds_x ----- 19

- Figure 44 - Flow of Air in Smooth Tubes (effect of initial turbulence) - ratio of friction factors versus X/D ----- 21
- Figure 45 - Flow of Air in Smooth Tubes (effect of initial turbulence) - $\log f$ versus $\log \text{Reynolds}_x$ ----- 21
- Figure 46 - Flow of Water in Smooth Tubes (effect of initial turbulence) - ratio of friction factors versus X/D ----- 21
- Figure 47 - Flow of Water in Smooth Tubes (effect of initial turbulence) - $\log f$ versus $\log \text{Reynolds}_x$ ----- 21
- Figure 48 - Flow of Water in Smooth Tubes (effect of initial turbulence) - ratio of friction factors versus X/D ----- 21
- Figure 49 - Flow of Water in Smooth Tubes (effect of initial turbulence) - $\log f$ versus $\log \text{Reynolds}_x$ ----- 21
- Figure 50 - Flow of Air in Smooth Tubes (effect of initial turbulence) - ratio of friction factors versus X/D ----- 21
- Figure 51 - Flow of Air in Smooth Tubes (effect of initial turbulence) - $\log f$ versus $\log \text{Reynolds}_x$ ----- 21
- Figure 52 - Flow of Air and Water in Smooth Tubes (effect of apparatus) - ratio of friction factor versus X/D - no induced turbulence -21
- Figure 53 - Flow of the Air and Water in Smooth Tubes (effect of apparatus, no induced turbulence) - $\log f$ versus $\log \text{Reynolds}_x$ -22
- Figure 54 - Flow of Water in Smooth Tubes (two runs at same Reynolds Number, discrepancy) - $\log f$ versus $\log \text{Reynolds}_x$. ----- 22
- Figure 55 - Flow of Air and Water in Smooth Tubes (effect of apparatus) - ratio of friction factors versus X/D ----- 22
- Figure 56 - Flow of Air and Water in Smooth Tubes (effect of apparatus) - $\log f$ versus $\log \text{Reynolds}_x$ ----- 22

- Figure 57 - Flow of Air and Water in Smooth Tubes
(effect of apparatus, screen at inlet) -
ratio of friction factors versus X/D ----- 22
- Figure 58 - Flow of Air and Water in Smooth Tubes
(effect of apparatus, screen at inlet) -
 $\log f$ versus $\log \text{Reynolds } X$ ----- 22
- Figure 59 - Flow of Water in Smooth Tubes (no Initial
turbulence) - ratio of friction factors
versus X/D ----- 23
- Figure 60 - Supersonic Flow of Air in Smooth Tubes -
ratio of friction factors versus X/D ----- 24

I.

ABSTRACT

The apparent friction factor for incompressible flow in the first forty diameters of smooth straight tubes was determined, with emphasis on the initial turbulence. Reynolds number based on the diameter, and the length-diameter ratio. Reynolds numbers ranged from 38,910 to 587, 890. Tube size ranged from .373 inches to 4,000 inches.

Friction factors for flow with no induced turbulence ranged from 1/4 to 3 times that for fully developed flow. Friction factors for flow with induced turbulence ranged from 1/6 to 15 times that for fully developed flow. Values of friction factors for fully developed flow agreed with those from the Karman-Nikuradse equation.

A definite change of regime, similar to the change from laminar to turbulent boundary layer on flat plates, was noticed. With no induced turbulence the transition from laminar to turbulent started at values of Reynolds_x equal 550,000 (X/D equal 2 to 12) and the transition was complete at values of Reynolds_x of 1×10^6 (X/D equal 2 to 16). These values of Reynolds number in agreement with those for flat plates, signify that for low Reynolds number flows the transition will take place at higher values of X/D than for high Reynolds numbers. As in the case of the Karman-Nikuradse equation, value of friction factor were seen to decrease with increasing Reynolds number.

With a screen at inlet, no violent change of regime takes place. Rather a change of slope in the friction

factor versus Reynolds number curve appears to take place at Reynolds number (based on length) of 800,000. In these runs, the friction factor is consistently 2 to 15 times that of Karman-Nikuradse. Flow is seen to change in character at lower values of X/D for higher Reynolds numbers. Friction factors decrease with increase of Reynolds number.

A comparison of runs on two sets of apparatus at the same Reynolds number reveals that taking fluid from essentially stagnation conditions gives a large deviation in the friction factor compared to that for flow with a calming chamber at inlet. Present results indicate that values of friction factor for flow from a good calming chamber may be of the order of 3 times those obtained with flow from stagnation conditions.

Agreement with results of other investigators is quite good, values of transition points checking rather well.

II.

PURPOSE

The purpose of this investigation was to determine the apparent friction factors for incompressible flow through a length of smooth round pipe with particular attention to the entrance region in which the velocity distribution changes from the constant velocity distribution across the inlet section to the fully developed turbulent condition. Especial interest was focused upon the effects of initial turbulence, Reynolds number, and length-diameter ratio.

III.

STATUS OF THE PROBLEM

Recent advances in the field of hydro- and aeromechanics have focused considerable attention on the problems of turbulent flow of fluids, both compressible and incompressible, through pipes, tubes, ducts, and over surfaces where the flow does not reach the fully developed turbulent condition. One might cite as examples the flow of fluids through the induction systems of gas turbines, jet propulsion units, superchargers, through short tubes and pipes of pumps, turbines, heat exchangers and so forth.

Friction factors for such flow near the entrance of a tube, into which is introduced a stream of uniform velocity, are affected by the changes in velocity profile which are known to take place in incompressible flow in the first thirty to fifty pipe diameters. Normally these friction factors are calculated on the basis of a constant velocity distribution across all sections. This ignores the momentum transfer which takes place with changing velocity profiles, and hence cannot be the true friction factor defined as $\frac{C_f}{\rho V^2}$, where τ_0 is the shear stress at the wall. As contrasted with this "true friction factor", these values will be called the "apparent friction factor".

The "true friction factor" and the "apparent friction factor" must needs coincide when there is no change of velocity profile. This occurs near thirty pipe diameters

from the entrance where the familiar Karman-Nikuradse relation

$$\frac{1}{\sqrt{4f}} = -0.8 + 2 \log (\text{Re} \sqrt{f})$$

where f is the friction factor, and Reynolds the Reynolds Number, applies to give the pressure drop. Measurements of friction factors in the inlet section of straight tubes indicate that values of f in this inlet section may range more than 100 per cent higher than those corresponding to the Karman-Nikuradse formula. It can thus be seen that for short lengths of flow very serious errors may be made.

The earliest indication of variation of friction factors near the entrance of straight tubes comes from Kirsten (13) who measured velocity distributions at various values of X/D (X being the distance from the entrance, D the tube diameter) and in a range of Reynolds Number from 20,000 to 80,000 for air flow at low Mach Number. Included were calculations of apparent friction factor for two runs the results of which indicate that the apparent friction factor at very low values of X/D was considerably higher than that for fully developed turbulent flow, but that as X/D increased the friction factor dropped below the values for fully developed flow, and suddenly increased to values above the fully developed value and slowly decreased until near $30 X/D$ it was substantially the fully developed value.

Brooks, Craft, and Montrello (14), measured apparent friction factors in the entrance region of a tube in which water was flowing (range of Reynolds number 40,000 to

200,000). They too found marked variation of friction factor with X/D , somewhat similar to that reported by Kirsten, but in poor agreement as regards magnitude.

Somewhat similar results were obtained by Keenan and Newmann for supersonic flow (12) but as yet there exists no correlation between apparent friction factor, X/D , and Reynolds Number.

In view of discrepancies observed in values of "apparent friction factor" divided by "true friction factor" for fully developed flow, the present thesis program was proposed. Kirsten (13) mentions the effect of installing calming devices, and since the approach velocity in the work of Brooks, Craft, and Montrello was rather high, it was proposed to install a calming chamber and reduce the initial turbulence as much as practicable. This done, the proposal was to vary both tube size and initial turbulence to determine their effects upon the apparent friction factor in the inlet length.

From the data of Kirsten (13) on velocity profiles, and the work of Wang (11) which predicts velocity profiles in marked agreement with Nikuradse's experiments, an estimate of the change in momentum flux with X/D might be made and from this the apparent friction factor adjusted to the true friction factor (14).

IV.

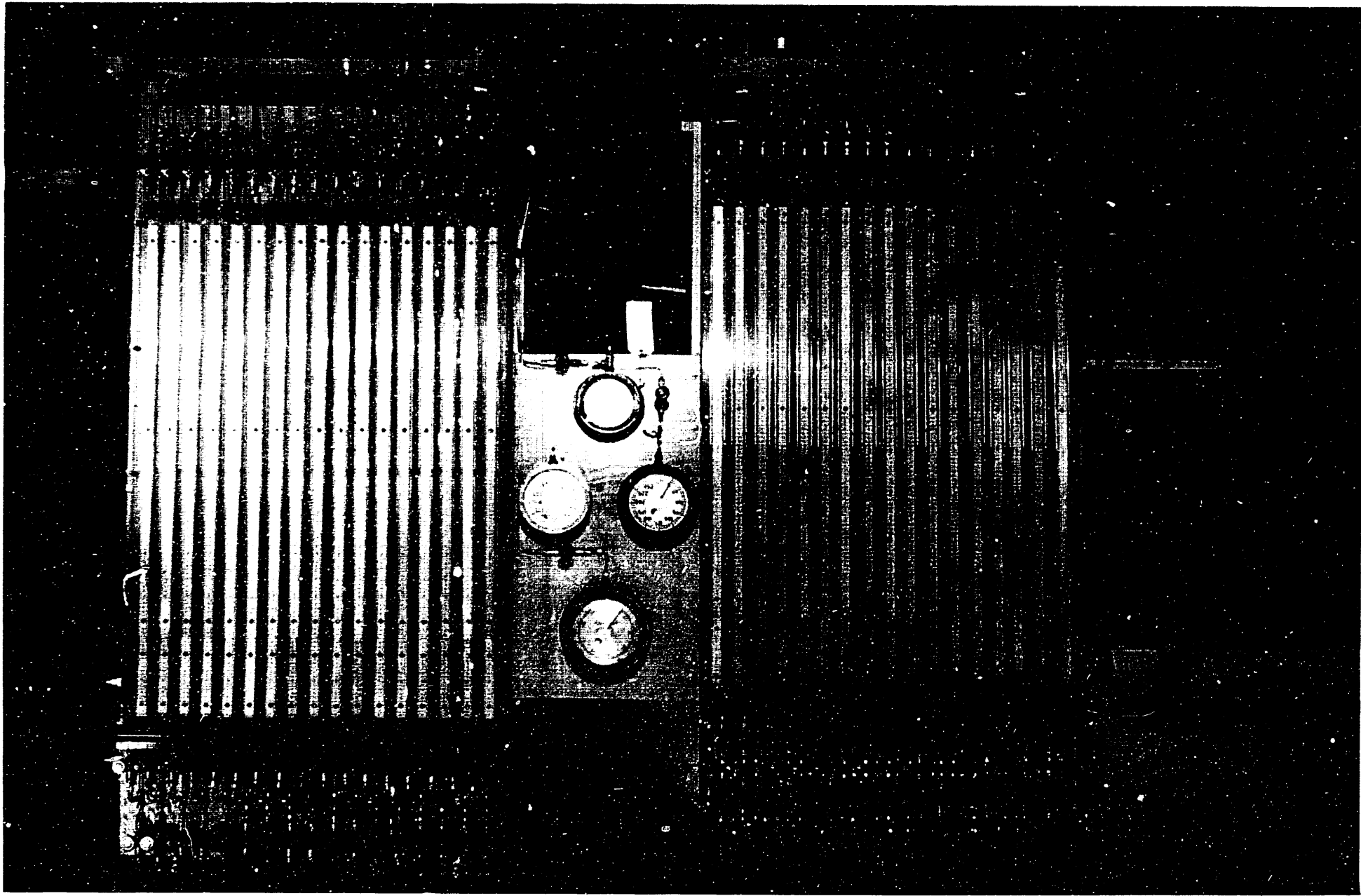
CHOICE AND DESCRIPTION OF METHODS

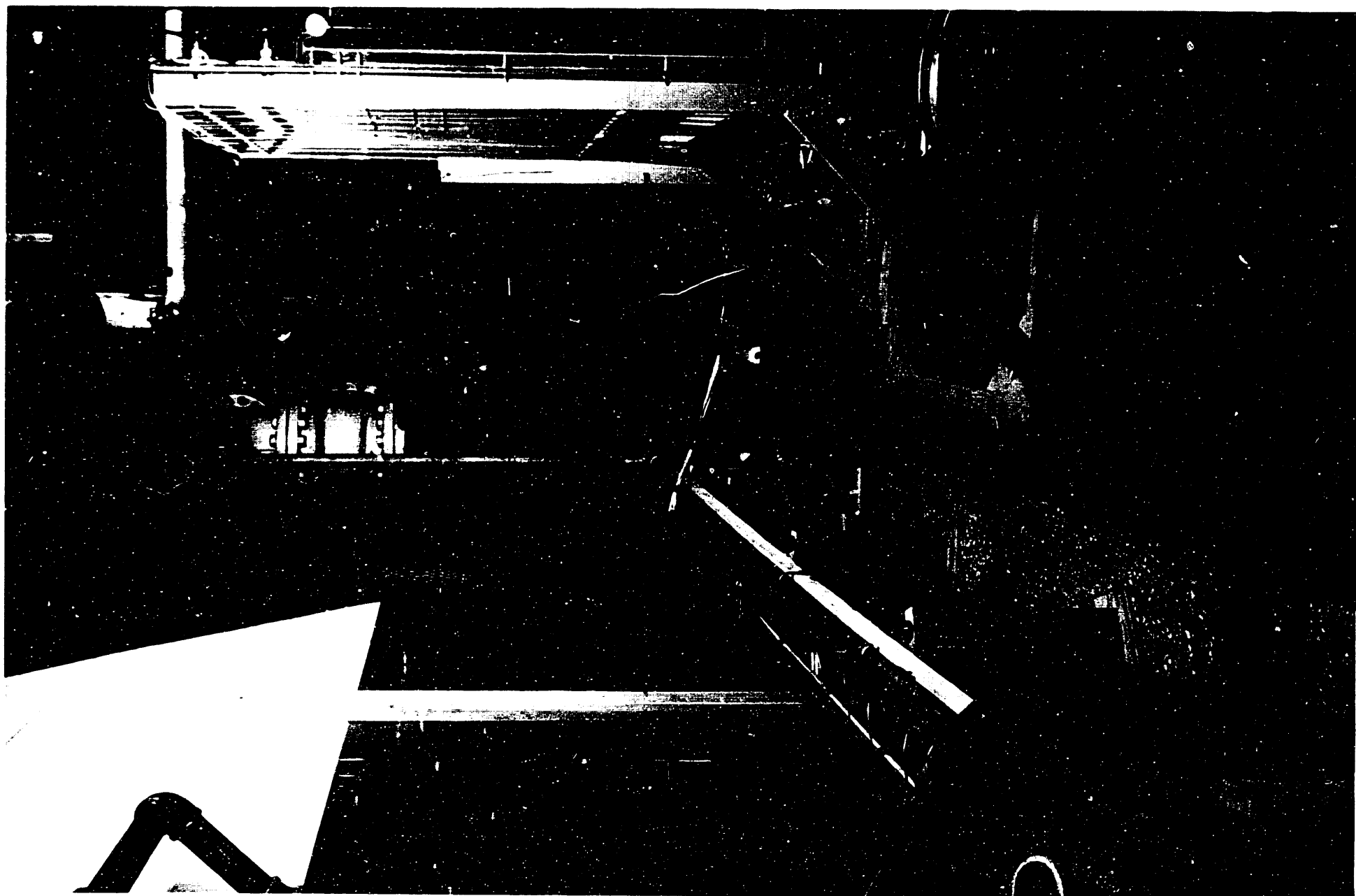
The problem of experimental investigation was one of measuring pressure differences along the length of straight tubes through which a fluid flowed. In one case the fluid was air, in the other, water. To all practical intents and purposes each type of experiment was separate and will be described.

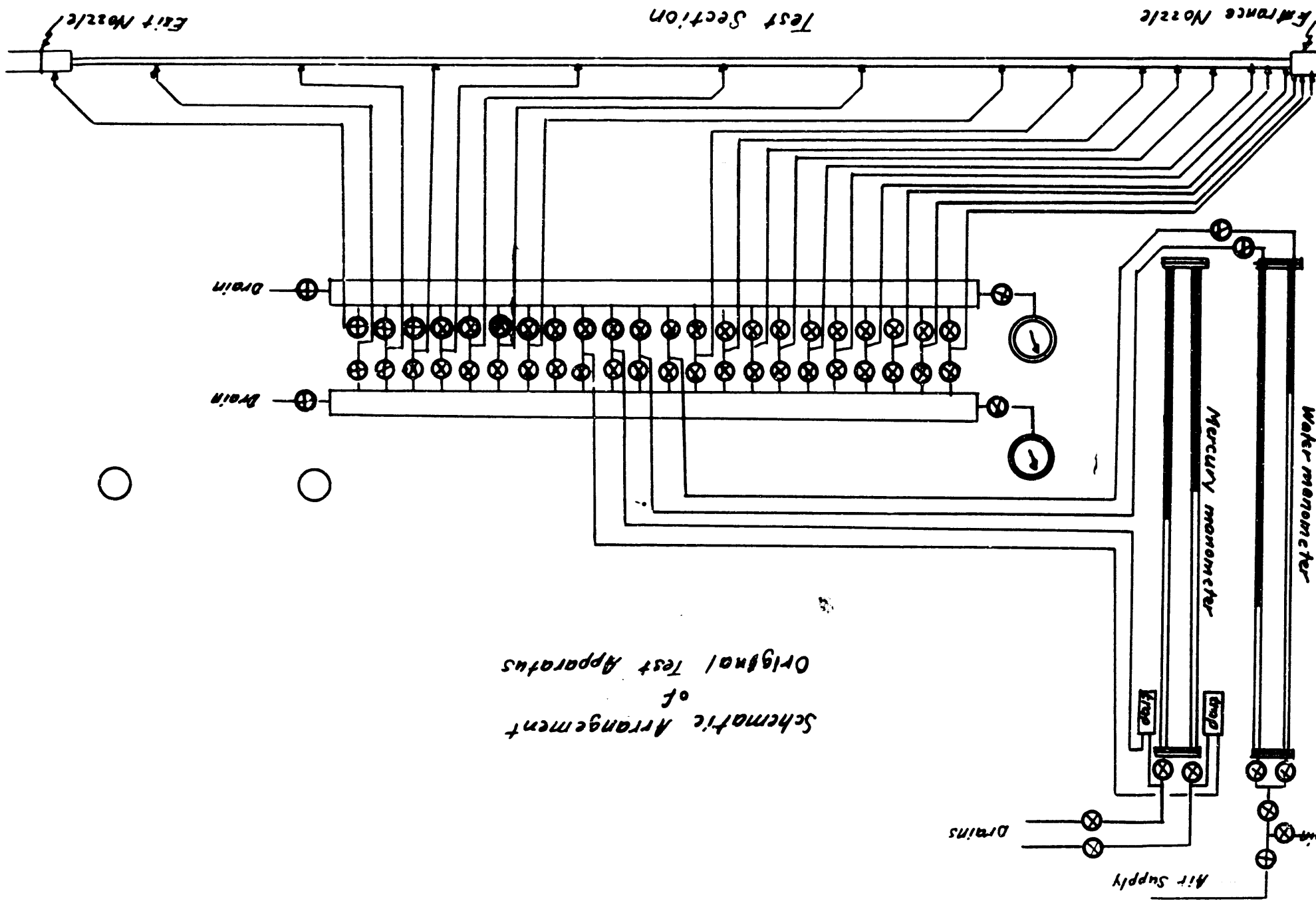
A. Tests with air.

In the tests involving air flow, it was desired that all pressured readings be taken at one time. However, the pressure drop from point to point in the tube was of such a magnitude that the use of simple U-tube manometers was impossible, and the only feasible measuring device was the micro-manometer. Therefore, it was no longer simple to measure all pressures simultaneously.

In view of these separate pressure measurements, the following method was devised. Two Chattock micromanometers were utilized so that the pressure at the desired section could be determined, as well as a base pressure, the pressure at the inlet section. The pressure at the inlet section, a direct function of the flow, allowed maintenance of a steady flow rate, the difference in readings of the micro-manometers yielded the pressure drop down the tube, and a sharp-edge orifice and its manometer adjuncts allowed a calculation of the flow velocity. The other necessary quantities were derived from measurement of room conditions.







Schematic Arrangement
of
Original Test Apparatus

Figure 1

Initial turbulence was not measured, but used qualitatively.

B. Tests with water.

The original pressure measuring equipment for the water flow tests consisted of both a U-tube mercury manometer and a water manometer. These manometers (figure 1) were manifolded to 18 pressure taps in such a way that separate readings of both the water and mercury manometers could be taken across any pair of taps. In addition, as a precaution against leakage, the manometer connections could be reversed and additional readings taken.

The method of operation was to take a reading between a pair of taps with the mercury manometer, and to reverse the connections through the manifolds, and re-read the mercury manometer. Before each reading of the mercury manometer, water was bled from the pressure lines to purge any trapped air. The water manometer, read next, also was bled to purge all air, and then high pressure air used to force the levels down to the reading range. Again connections were reversed, the pressure lines purged, and air applied to attain another reading.

Each complete set of readings across one pair of taps required four separate purging operations, the bleeding of a total of eight lines. The large volume of water to be bled, the pressure tap size (.020 inch) combined to require the greater part of a day for each complete run.

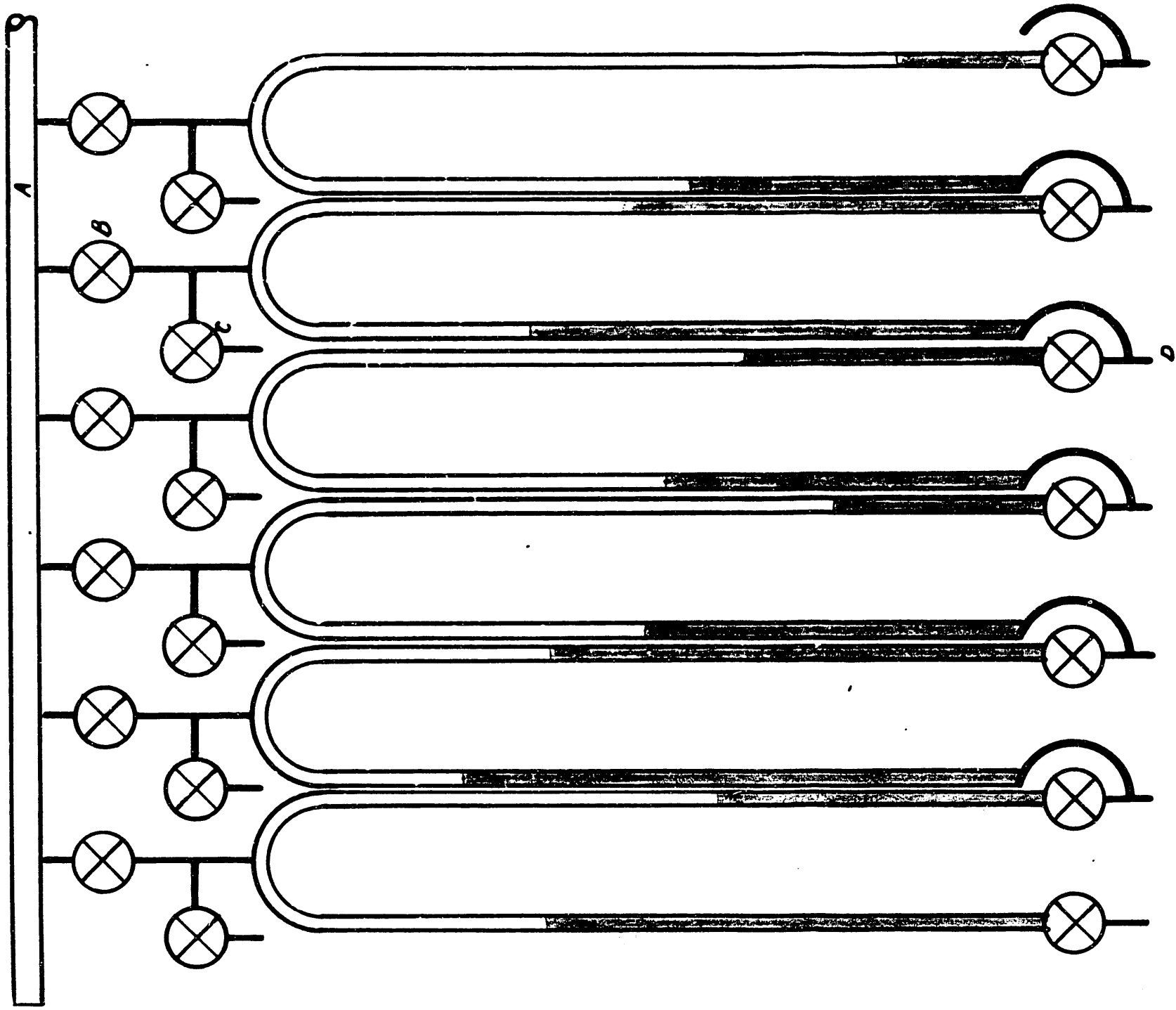
The only advantage of this original system was that each pressure tap could be used in combination with any

simultaneous readings were possible, and the flow-rate being difficult to maintain, numerous corrections had to be applied to the original data.

With this background a new pressure measuring system was devised. This system constituted a series of U-tube manometers as did the old. For high flow rates, a mercury manometer, and for low flow rates, a water manometer were to be provided across pressure taps n and $n+1$ so that simultaneous pressure readings could be taken across successive pairs of taps. The velocity of flow was to be determined by measuring the time required for a measured weight of water to flow. The other measured quantity was the temperature, so that the density and viscosity could be determined.

The other changes in the original equipment were designed primarily to insure smooth flow conditions at the inlet to the test section. The desire was to reduce the approach velocity in proportion to the flowing stream velocity, and to reduce the initial turbulence insofar as practicable. Thus a relatively large calming chamber (figures 4 to 8) was designed and equipped with plates, honeycomb, and mesh screen to carry this out.

Having thus reduced the initial turbulence, it was desired in some runs to induce turbulence. This was to be accomplished by the installation of various sized screens at the outlet section of the calming chamber.



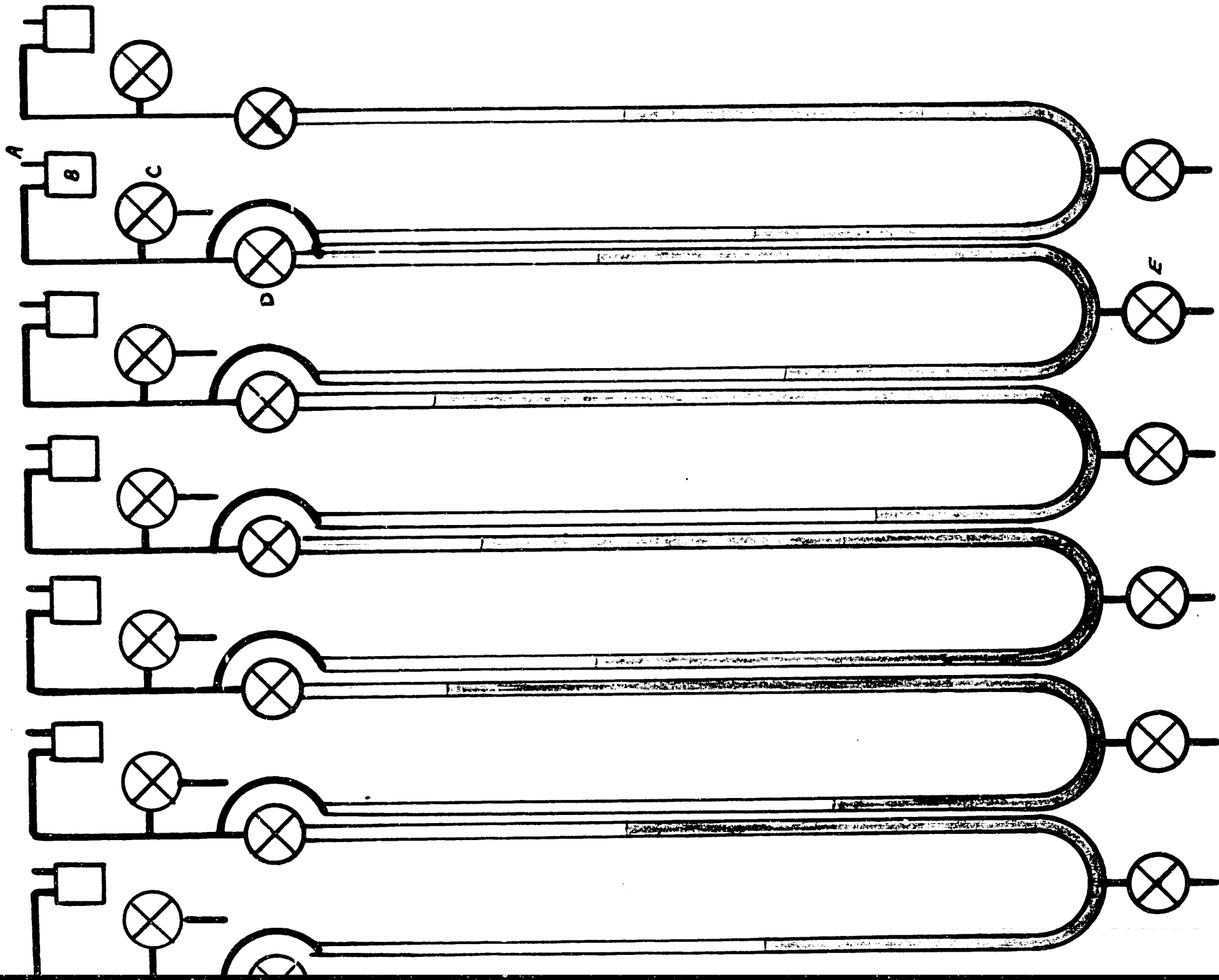
*Schematic Diagram
of*

Water Manometer Panel

A. air manifold

B. air valve

C. bleed valve



Schematic Diagram

Mercury Manometer Panel

- A. pressure connection*
- B. mercury trap*
- C. A bed valve*

Figure 4

Calming Chamber Assembly
1 1/2" = 1'

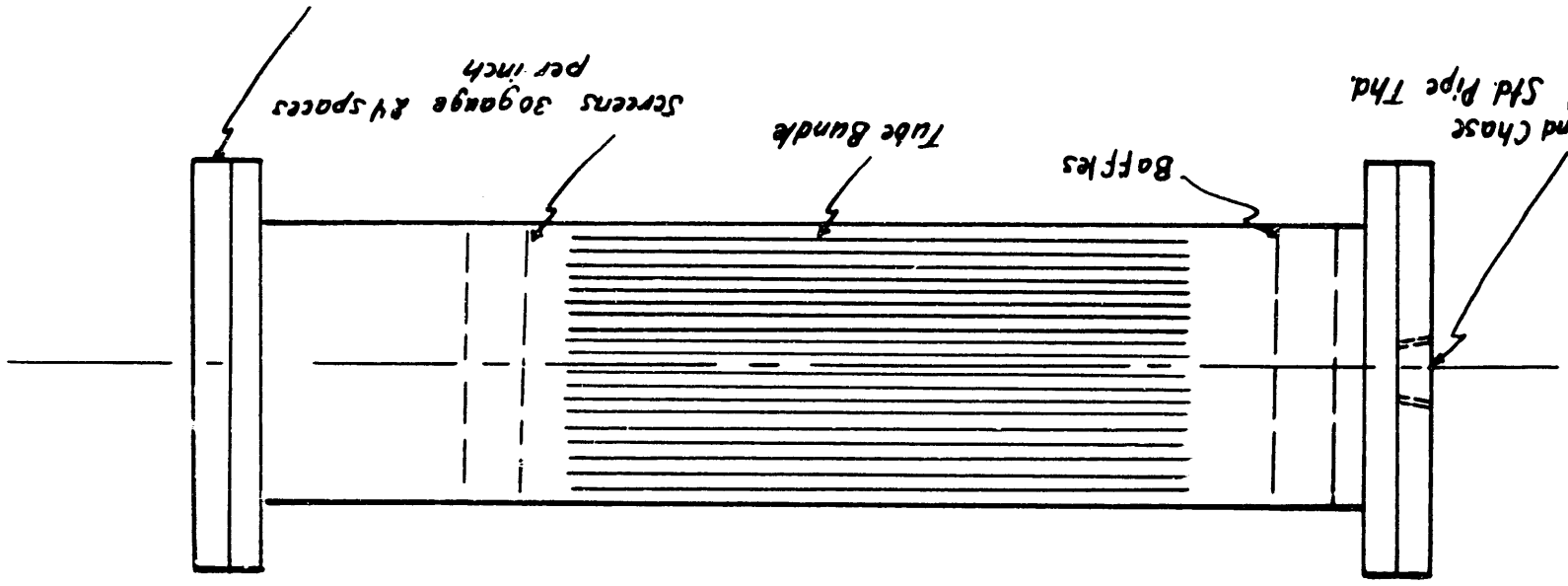
see calming chamber flange detail

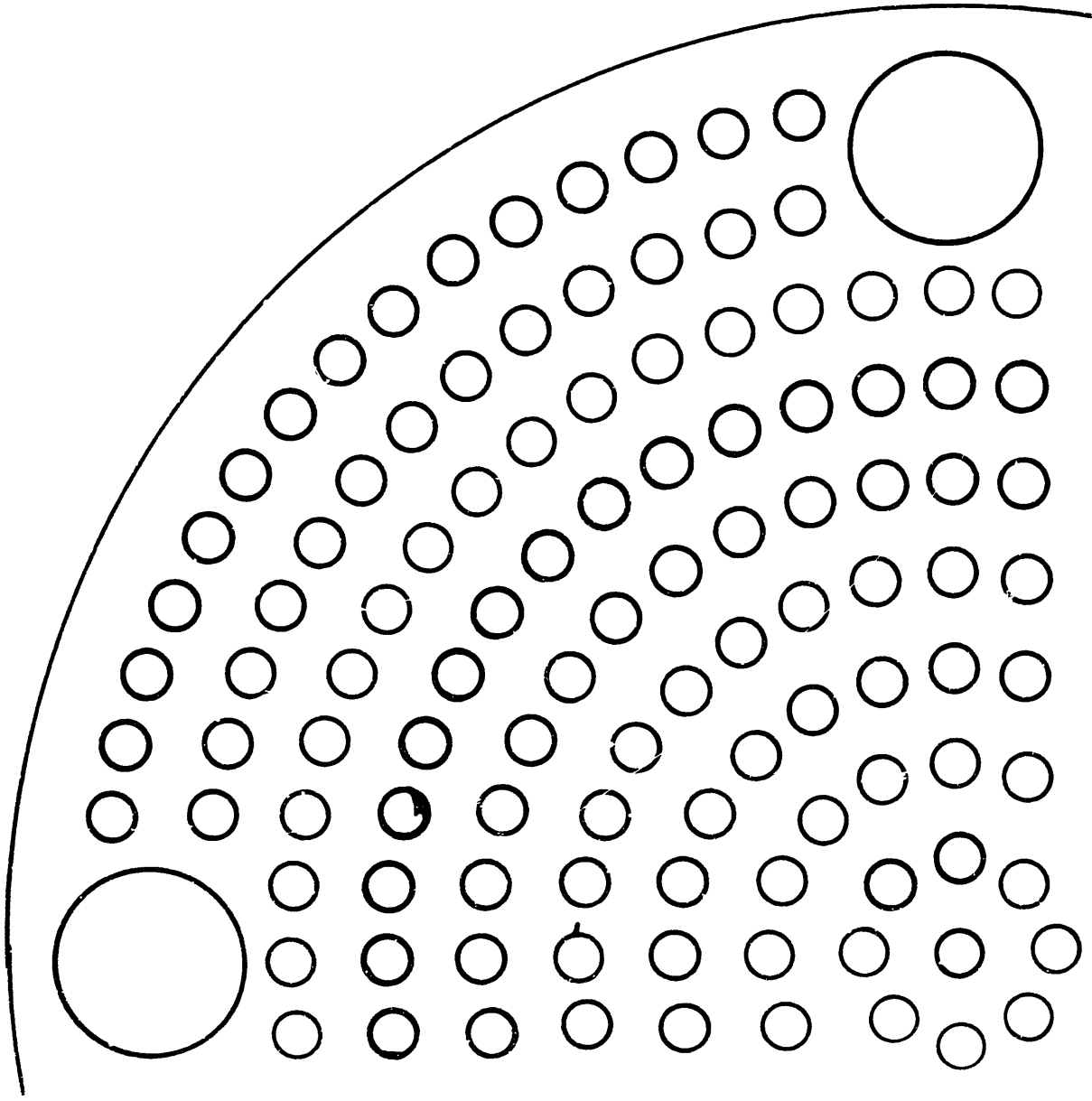
Screens 30 gauge & 4 spaces
per inch

Tube Bundle

Baffles

Drill and Chase
2 1/2" Std Pipe Thd.



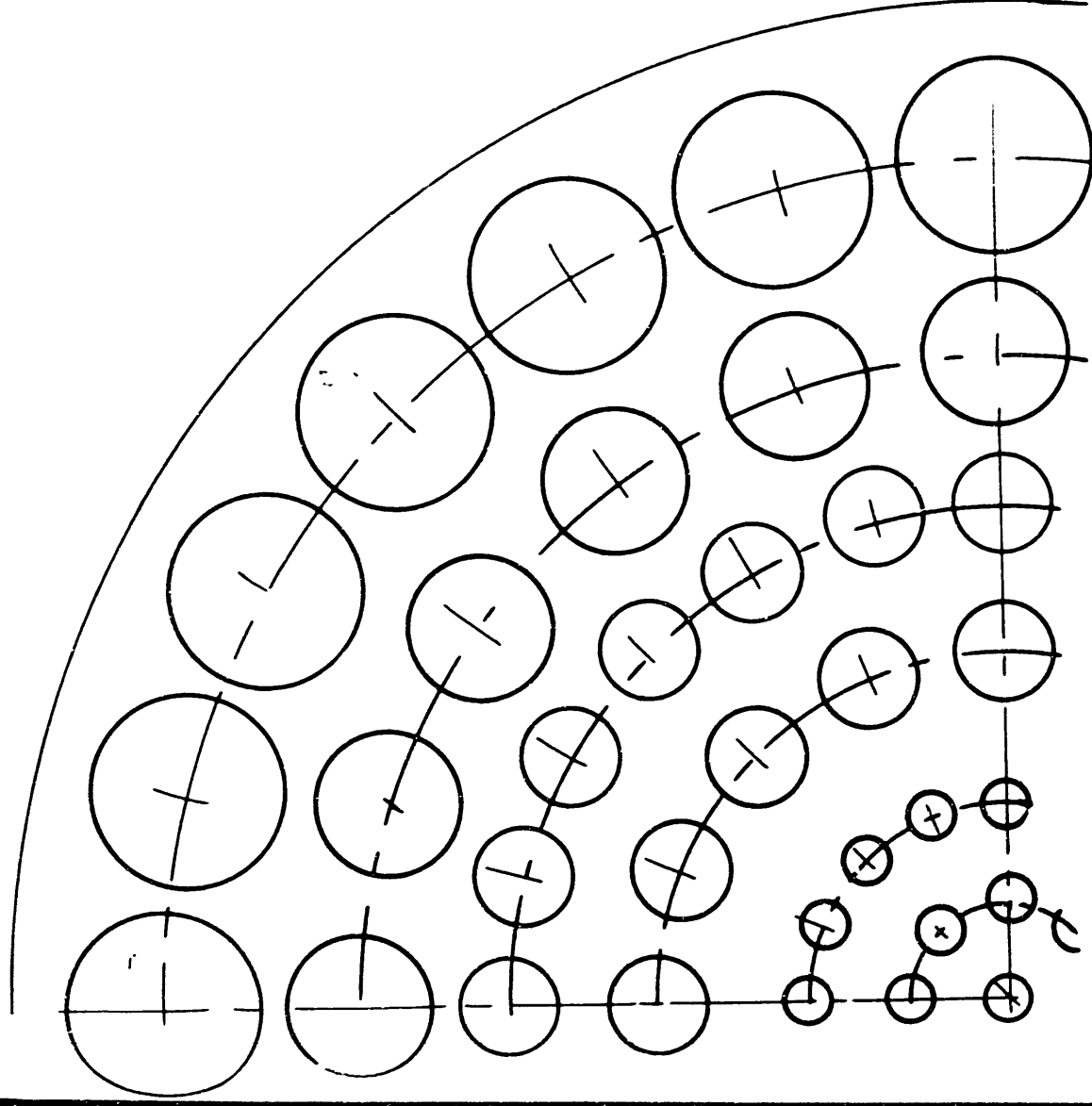


Brass plate, 10" diameter, 1/8" thick

Schedule of holes:

Dia. of pitch circle	No. of holes	Dia. of holes
0	1	1/4
1	8	1/4
2	16	1/4
3	24	1/4
4	32	1/4
5	40	1/4
6	48	1/4
7	56	1/4
8	52	1/4
8 1/2	4	1
9	60	1/4

Distributor Baffle for Calming Chamber



Brass plate, 10" diameter $\frac{1}{16}$ " thick

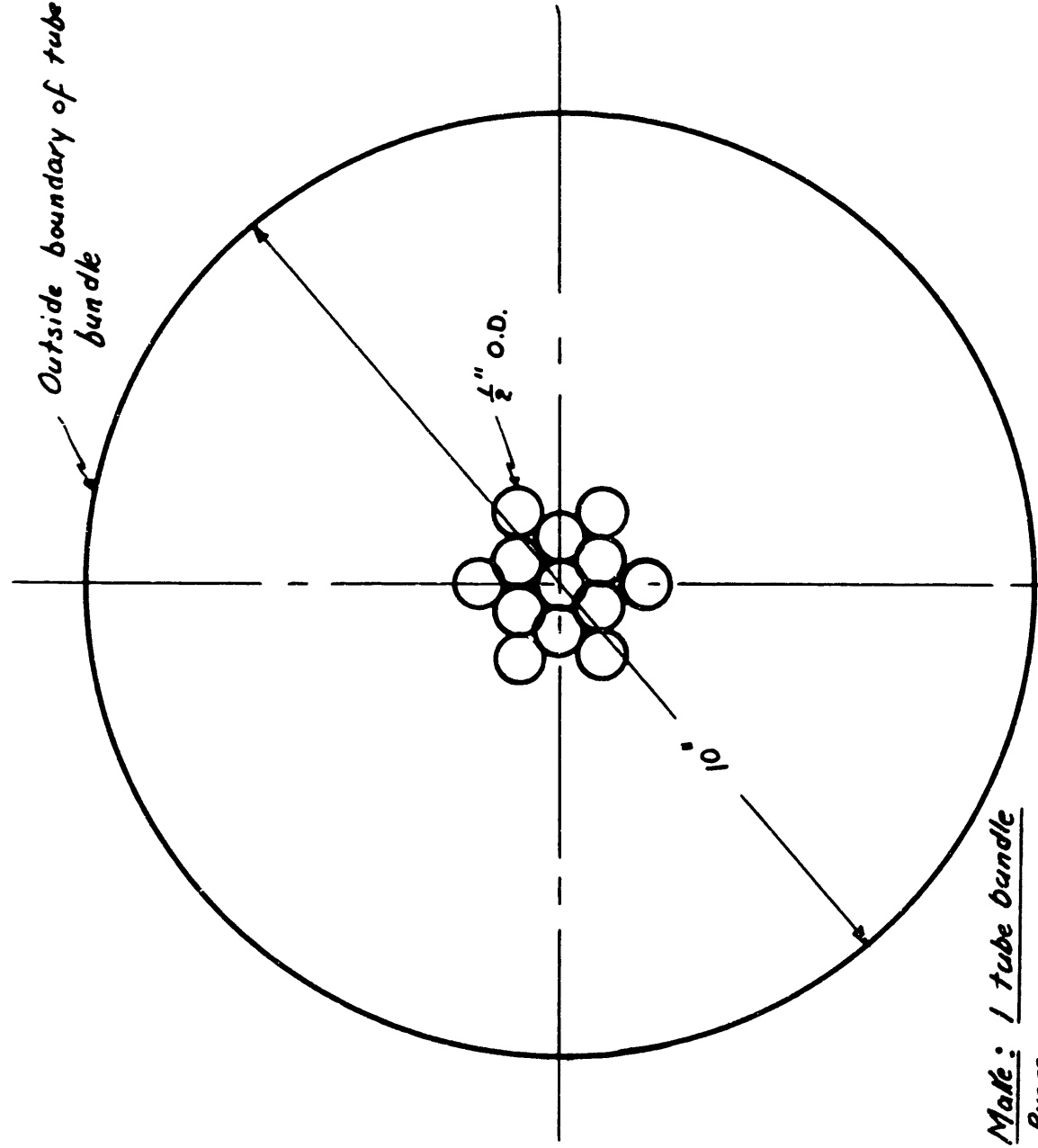
Schedule of holes:

Dia. of pitch circle	No. of holes.	Dia. of holes
0"	1	$\frac{1}{4}$ "
1	8	$\frac{1}{4}$ "
2	16	$\frac{1}{4}$ "
$3\frac{1}{2}$	16	$\frac{1}{2}$ "
5	24	$\frac{1}{2}$ "
$6\frac{1}{2}$	20	$\frac{3}{4}$ "
$8\frac{1}{2}$	24	1"

Distributor Baffle for Calming Chamber
Scale ~ Full Size

Honeycomb for Calming Section

Bundle of $\frac{1}{2}$ " brass tubes, $23\frac{7}{8}$ inches long.
Outside diameter of bundle, 10 inches.



Make: 1 tube bundle
Brass.

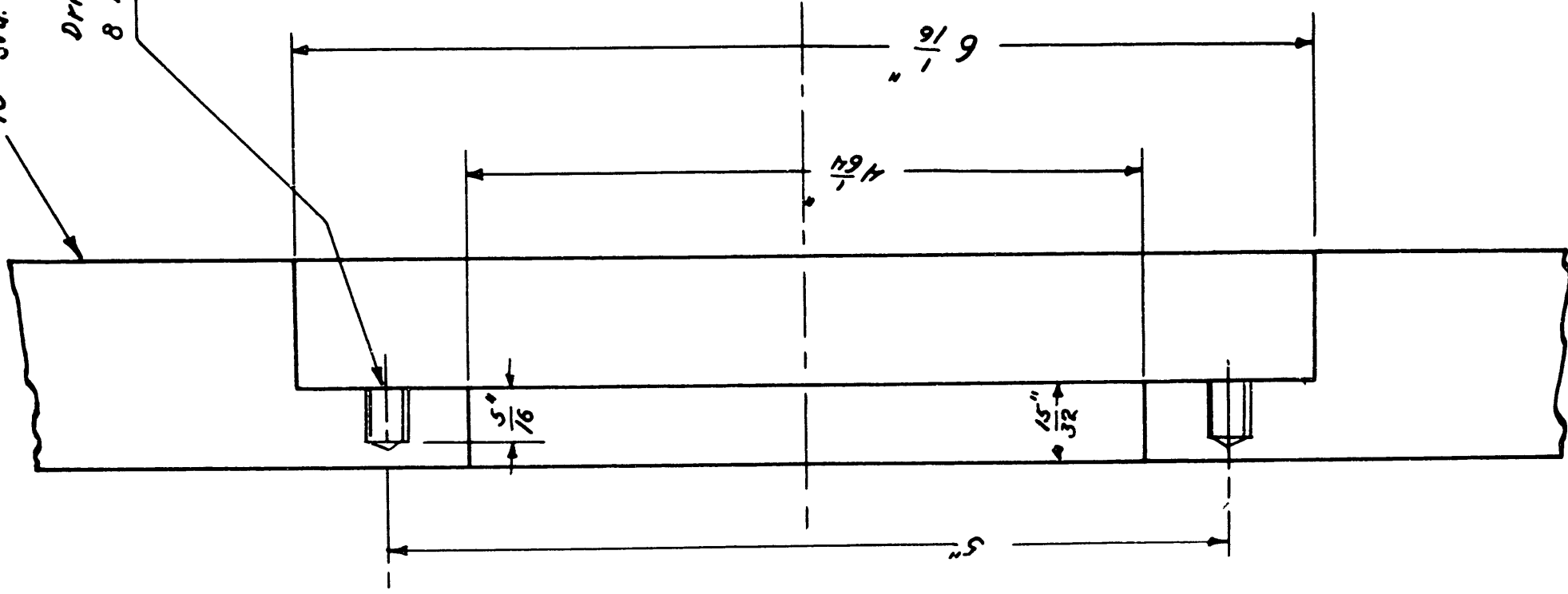
Cut $\frac{1}{2}$ " tubing to $23\frac{7}{8}$ " length and remove burrs from ends. Tin ends of tubes with solder for about 2 " of length. Pack tubes in circle 10 " diameter, with ends squared off, and heat ends with torch so solder runs and joins tubes together.

Scale: Half Size

10" Std. C. I. Pipe Flange

Drill & tap for $\frac{1}{4}$ " cap screws
8 holes evenly spaced on 5" B.C.

Furnish 8 - $\frac{1}{4}$ " cap screws
with hex. heads, $\frac{1}{2}$ " under head



FLANGE OF
CALMING CHAMBER